Journal of The Electrochemical Society, **153** (8) G765-G770 (2006)
0013-4651/2006/153(8)/G765/6/$20.00 © The Electrochemical Society

Fabrication of Pyramidal Patterned Sapphire Substrates for High-Efficiency InGaN-Based Light Emitting Diodes

D. S. Wuu,[a,b,z] W. K. Wang,[a] K. S. Wen,[a] S. C. Huang,[a] S. H. Lin,[b] R. H. Horng,[c] Y. S. Yu,[d] and M. H. Pan[d]

[a]*Department of Materials Engineering, National Chung Hsing University, Taichung 402, Taiwan*
[b]*Department of Materials Science and Engineering, National Fomosa University, Huwei 632, Taiwan*
[c]*Institute of Precision Engineering, National Chung Hsing University, Taichung 402, Taiwan*
[d]*Wafer Works Corporation, Research and Development Division, Taoyuan 326, Taiwan*

In this study, a wet-etched pyramidal patterned sapphire substrate (PSS) was used to fabricate the near-ultraviolet InGaN-based light-emitting diodes (LEDs). The pyramidal PSS was etched using a $3H_2SO_4$:$1H_3PO_4$ mixture solution and the activation energy of this reaction is determined to be 28.2 kcal/mol. Three symmetric sidewall facets of the etched pyramidal hole were $\{11\bar{2}\bar{k}\}$ on the (0001) sapphire. It was found that the GaN epi layer grew laterally from the top of the pyramid pit and overhung the cavity. An evident reduction in dislocation density of the GaN-on-PSS sample can be confirmed by the etch-pit-density, double-crystal X-ray, and micro photoluminescence measurement results. Under a 20 mA forward injection current, the output power of the conventional and pyramidal PSS LEDs (in epoxy lamp form, λ_D = 400 nm) were 7.45 and 9.35 mW, respectively. A 25% enhancement in output power was achieved in the pyramidal PSS LED as compared with that of the conventional LED sample. The enhanced output power is not only due to the improvement of the internal quantum efficiency upon decreasing the dislocation density, but also due to the enhancement of the extraction efficiency using a pyramidal PSS. From light-tracing calculation, the pyramidal reflector arrays can offer more probability of escaping photons from the GaN/sapphire interface, resulting in an increase in light extracting efficiency.
 [DOI: 10.1149/1.2209587]

Manuscript submitted February 28, 2006; revised manuscript received April 17, 2006. Available electronically June 15, 2006.

Recently, tremendous progress has been achieved in nitride-based semiconductor materials. The high emission InGaN light-emitting diodes (LEDs) have become commercialized products between the ultraviolet (UV) and green spectra region, which attracted considerable application in the areas of photonic devices, such as traffic light, outdoor full color displays, and solid-state lighting. Currently, the most commonly used method to achieve white-light LEDs is to combine an yttrium-aluminum-garnet phosphor wavelength converted with a GaN blue LED chip. The UV LEDs can be used as an efficient pumping source for developing white-light LEDs to solve the low color-rendering-index problem.[1] To enhance the light extraction efficiency, the patterning or roughening of the surface of GaN-based LEDs have been reported.[2-4] However, UV LEDs are more sensitive to dislocation than blue LEDs, as indicated from previous studies.[5] It is well known that a dislocation density in the order of 10^9 to 10^{11} cm^{-2} is inherent in the epitaxial GaN films on sapphire substrates due to the large lattice mismatch.[6,7] High dislocation density will influence the device characteristics, such as device lifetime, electron mobility, and the quantum efficiency of radiative recombination. Therefore, how to further reduce the dislocation density is an important issue for fabricating high-performance UV LEDs.

Many different growth approaches have been proposed for threading dislocation density reduction.[8-16] Lateral epitaxial overgrowth is a commonly used technique utilizing metallorganic chemical vapor deposition (MOCVD) to reduce the threading dislocation (TD) density to the 10^7 cm^{-2} range. In this method, a GaN epi layer, several micrometers in thickness, is first grown onto a sapphire substrate. Subsequently, a SiN_x or SiO_2 strip type mask is produced, followed by epitaxial growth.[8-11] These approaches suffer from the complex MOCVD re-growth process, resulting in a lower production yield. Several groups have recently demonstrated direct lateral epitaxy growth onto stripe-type patterned sapphire substrates (PSSs). Tadatomo et al. have adopted models of parallel grooves along the $(11\bar{2}0)$ sapphire to fabricate nitride LEDs.[12,13] Chang et al. have described the use of parallel stripes along the sapphire $(1\bar{1}00)$ direction for their blue LED growth.[14] In our previous studies, a considerably improved output power of InGaN-based UV LEDs on PSSs was obtained.[15,16] The PSS was prepared using a periodic hole pattern on the (0001) sapphire with different etching depths. The proposed method can reduce the TDs via a single growth process without any interruption or deposition onto the SiO_2 mask. It also eliminates the need for a precise photolithography process to transfer a special pattern axis and prevents the induced contamination.

Although the PSS can be fabricated using a dry etching technique, there still exist some dry etch induced strain and damage on the sapphire surface,[17] which will limit further improvement of the LED epilayer quality. In this work, a systematic study of the PSSs using various H_2SO_4/H_3PO_4 mixture ratios was performed. Here we use a chemical wet etching method, instead of dry etching, to fabricate a PSS with periodic pyramidal holes. Details of the structure and optical properties of the 400 nm InGaN LEDs grown on the pyramidal PSS are described.

Experimental

The PSS used in this study was 2 in. 430 μm thick (0001) sapphire misoriented 0.2° off toward the $(1\bar{1}00)$. A low-pressure chemical vapor deposited SiO_2 layer was served as the wet etching mask. The pyramidal PSS was prepared using a periodic hole pattern with an etching depth (D_h) of 1.5 μm. The pyramidal hole array (3 μm diam and 3 μm spacing) was generated using standard photolithography process. Two kinds of acid solutions were chosen: 98 wt % H_2SO_4 and 85 wt % H_3PO_4. A mixture of H_2SO_4:H_3PO_4 (3:1) solution was used to etch sapphire substrate at 280°C. During the MOCVD growth, trimethylgallium, trimethylindium, and ammonia were used as the gallium, indium, and nitrogen precursors. Biscyclopentadienyl magnesium and disilane were employed as the p- and n-type dopant sources, respectively. The carrier gas was hydrogen through the growth except that nitrogen was used for the InGaN growth. Prior to the growth, sapphire substrates were thermally baked at 1100°C in hydrogen gas to remove surface contamination. The LED structure consisted of a 30 nm thick GaN low-temperature buffer layer, a 1.5 μm thick layer of undoped GaN, a 4 μm thick layer of n-type GaN:Si, an n-type $Al_{0.2}Ga_{0.8}N$/GaN layer, a multiple-quantum-wells (MQWs) active layer, a p-type $Al_{0.2}Ga_{0.8}N$/GaN superlattice layer, a 0.2 μm thick p-type GaN:Mg layer, and a 3 nm thick n^{++}-GaN tunneling layer. The LED sample used in this research had a chip size of 365 × 365 μm, fabricated using standard photolithography and dry etch techniques. The trans-

[z] E-mail: dsw@dragon.nchu.edu.tw

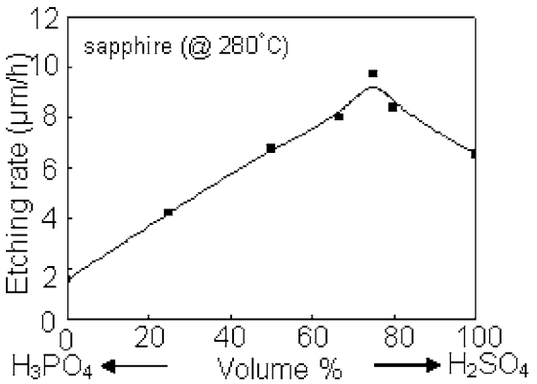

Figure 1. Etching rate of sapphire (0001) at 280°C as a function of the H_2SO_4:H_3PO_4 mixture ratio.

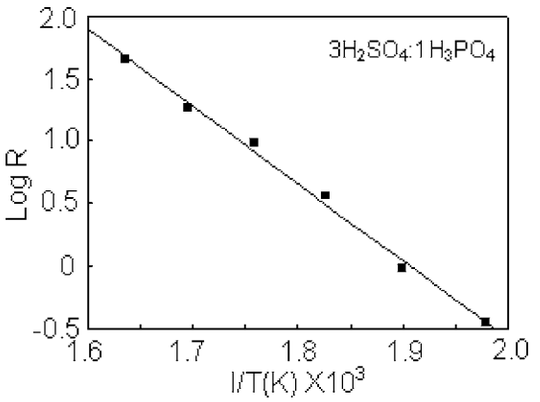

Figure 2. A semi-log plot of sapphire (0001) etch rate as a function of reciprocal temperature using a $3H_2SO_4$:$1H_3PO_4$ mixture solution.

parent indium-tin oxide layer and Ti–Al–Ti–Au were used as the p- and n-contacts, respectively. Note that the active layers in the normal and PSS LEDs were grown under the same growth run.

The surface morphology and microstructure were examined by field emission scanning electron microscopy (FESEM, JEOL 6700). The crystallinity of the as-grown GaN epi layers was examined using double-crystal X-ray diffractometer (Bede QC2A). The micro photoluminescence (μ-PL) was used to investigate the optical properties of the samples at room temperature using a He–Cd laser (325 nm) as an excitation source. Micro-Raman-scattering study was carried out using a 3D nanometer scale Raman system (Tokyo Instruments, Inc.). The laser beam focused on the sample surface is ~2 μm in diameter. The spectra were taken at room temperature with the excitation He–Ne laser (632 nm) in a backscattering geometry. The two-dimensional model of the candela map was simulated by the ray-tracing method using a Trace-Pro software. The output power of the LED lamp was also measured using an integrated sphere detector and the measured deviation was around 5% (Instrument Systems, CAS140B).

Results and Discussion

Figure 1 shows the etching rate of sapphire at 280°C as a function of the H_2SO_4:H_3PO_4 mixture ratio. It was found that the etching rate increased linearly when the H_2SO_4 volume ratio increased from 0 to ~ 75%. Because the etching process starts with the dissolution of the Al_2O_3 molecules into the acids as solvated Al^{+3} ions, the increase of the H_2SO_4 volume ratio will enhance the electrophilic attack of H^+ on the oxygen of Al–O–Al bridging moieties.[18] Further increasing the H_2SO_4 volume ratio results in the decrease of the etching rate. It is well known that the H_3PO_4 acts as a buffer agent in this mixture; the conjugate phosphate anions are significantly more nucleophilic than the corresponding sulfate ions and both the $Al(H_2PO_4)_3$ and $AlPO_4$ have a high solubility in H_3PO_4. When the H_2SO_4 volume ratio increased above 75%, the insoluble product of the $Al_2(SO_4)_3$ and $Al_2(SO_4)_3 \cdot 17H_2O$ became more dominant, which limited the etching rate of sapphire.[18] To calculate the activation energy of this reaction, the etching rate of *c*-plane sapphire as a function of reciprocal temperature from 220 to 320°C using a $3H_2SO_4$:$1H_3PO_4$ mixture solution was investigated and shown in Fig. 2. It is found that the etching rate can fit to a linear semi-log plot. The etching rate in micrometers per hole using a $3H_2SO_4$:$1H_3PO_4$ mixture solution can be given by

$$\log R_{3H_2SO_4:1H_3PO_4} = \frac{-6.17 \times 10^3}{T} + 12.98 \qquad [1]$$

where T is temperature is Kelvin and the R the etching rate. The activation energy of this reaction can be calculated to be 28.2 kcal/mol. A similar result was also obtained by Dwikusuma et al. in their surface treatment report.[18]

The evolution of the pyramidal PSS using a $3H_2SO_4$:$1H_3PO_4$ mixture solution at 280°C under different etching times was examined by FESEM as shown in Fig. 3. The (0001) etching facet was first observed onto the sapphire substrate at 5 min (Fig. 3a). As the etching depth increased, the (0001) facet decreased (Fig. 3b). The sapphire was kept $\{11\bar{2}k\}$ facets until the pyramid formation (Fig. 3c). The corresponding cross section micrograph of the etched pyramid was shown in Fig. 3d. Finally, the FESEM micrograph of the bare pyramidal PSS before MOCVD growth was shown in Fig. 3e. The formation of the crystallographic pyramidal patterns during the wet etching process can be attributed to the configuration of surface atoms and bond structure.[19,20] Figure 4 illustrates the sapphire

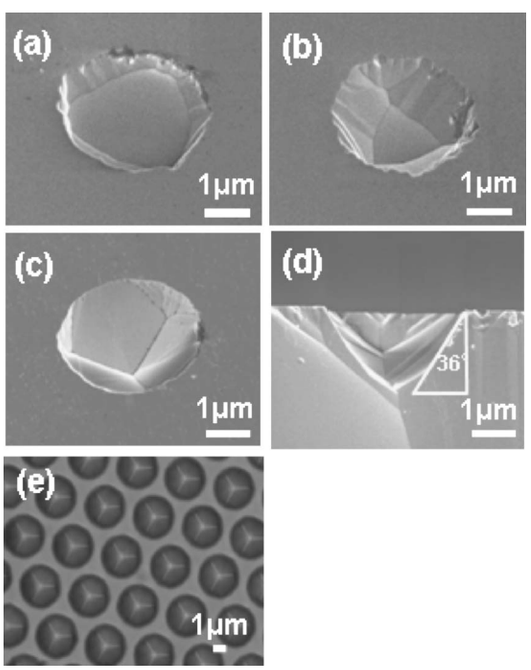

Figure 3. Time-dependent etching evolution of sapphire (0001) substrate using a $3H_2SO_4$:$1H_3PO_4$ mixture solution at 280°C: (a) appearance of (0001) etching facet at 5 min; (b) (0001) facet decreased at 15 min; (c) disappearance of (0001) facet until pyramid formation at 25 min; (d) cross section micrograph of pyramidal hole; and (e) pyramidal patterned sapphire substrate with a an etching depth of 1.5 μm before MOCVD growth.

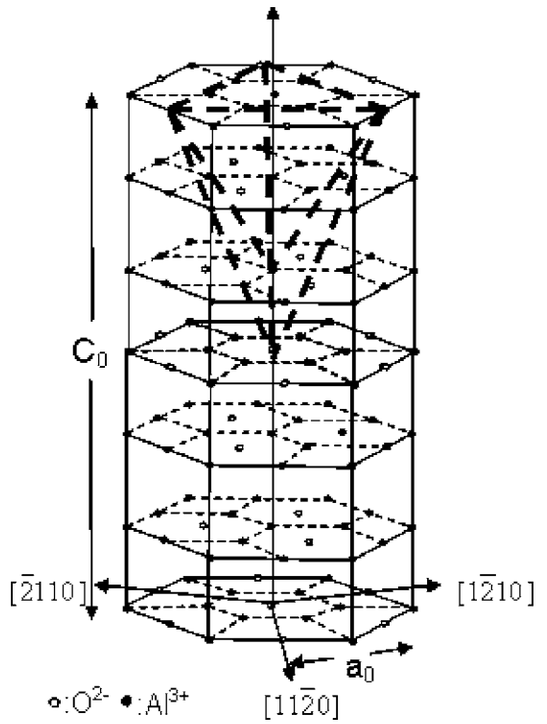

Figure 4. Illustration of sapphire (Al_2O_3) unit cell structural: Al atoms (filled circles) and O atoms (open circles).

(Al_2O_3) unit cell structural, where the filled circles label Al atoms, and open circles label O atoms. Generally, the lattice dimensions of sapphire were $a_0 = 4.748$ Å and $C_0 = 12.957$ Å, respectively. The $\{11\bar{2}\bar{k}\}$ sapphire facets composed of the pyramidal patterns, where k is an integer between 2 and 5 depending on the etching time. When the pyramidal pattern at the structural unit cell of sapphire was equal to $C_0/2$, the sidewall angle is 36.23°. The above calculation agrees well with the result of Fig. 3d, where the sidewall angle of the pyramid is about 36°and the three sidewalls of pyramid are symmetric (Fig. 3e).

Figure 5 shows the cross-section micrograph of a GaN epi layer grown on a pyramidal PSS using MOCVD. The periodic pyramidal pattern was not fully filled with the epilayer, where the GaN coalesced and laterally extended to from cantilever on the top of the

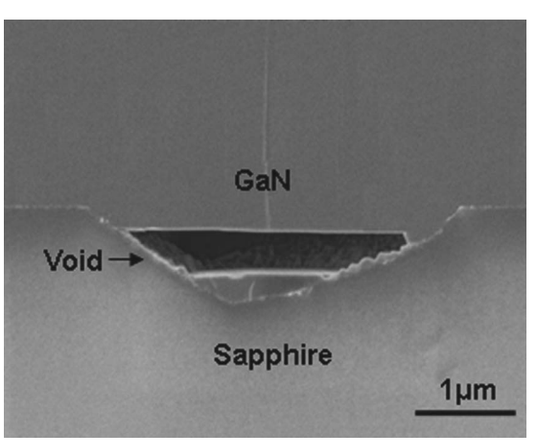

Figure 5. SEM cross section micrograph of a GaN epilayer grown upon a pyramidal patterned sapphire substrate.

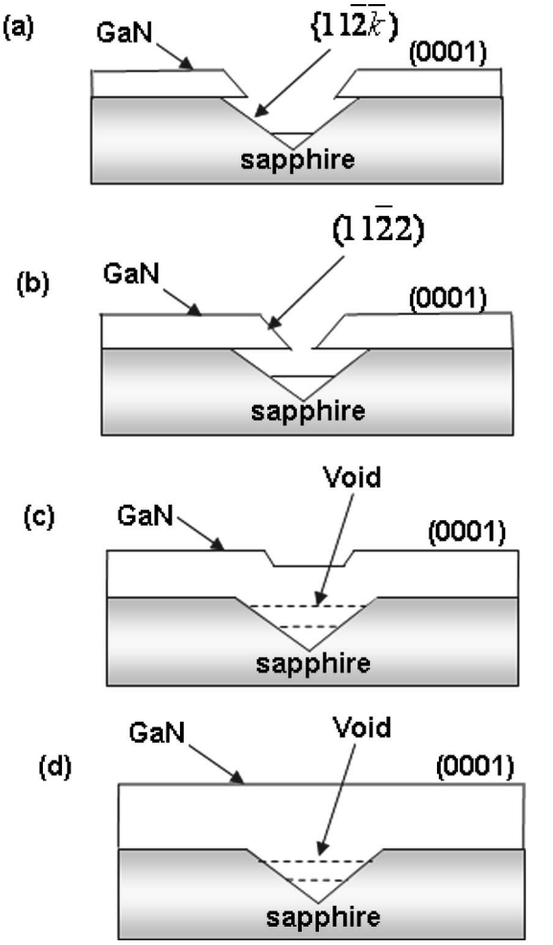

Figure 6. A schematic diagram of growth evolution of a GaN epi layer grown upon a pyramidal patterned sapphire substrate.

pyramidal hole. Therefore, the growth evolution of the GaN-on-PSS can be schematically shown in Fig. 6. A thin GaN (0001) epi layer was first grown onto a (0001) pyramidal PSS (Fig. 6a). The GaN also grew into the bottom and sidewall of the pyramidal pit. We have found that the GaN-on-PSS samples show the $\{11\bar{2}2\}$ facets during lateral overgrowth, as described in our previous study.[13] Several groups have also reported the $\{11\bar{2}2\}$ facets during lateral overgrowth.[21,22] Then the GaN epi layer grew laterally with new shape $(11\bar{2}2)$ facets (Fig. 6b). When the growth continued, the coalescence of the GaN occurred and the epitaxial lateral overgrowth was formed (Fig. 6c). Finally, a flat GaN epi layer was obtained on the pyramidal PSS with small voids (Fig. 6d).

Evidence of dislocation reduction in the GaN-on-PSS sample was obtained from the etch pit density (EPD) measurements where the n-GaN epi layers were chemically etched in a $1H_2SO_4$:$3H_3PO_4$ mixture solution at 260°C for 15 min. The EPD was around 1.5×10^9 cm^{-2} for an n-GaN epi layer on a conventional sapphire substrate (Fig. 7a) and decreased to 2.3×10^8 cm^{-2} for the GaN-on-PSS sample (Fig. 7b). This indicates that the dislocation reduction can be achieved via the lateral epitaxial overgrowth on a pyramidal PSS. The crystallinity of the GaN epi layer grown on a conventional sapphire and pyramidal PSS was examined by double-crystal X-ray diffraction. The corresponding full width at half-maximum (fwhm) of the (0002) X-ray rocking curves were 438 and 401 arcsec, respectively. The improvement in crystal quality examined by X-ray measurements showed in good agreement with the result revealed by

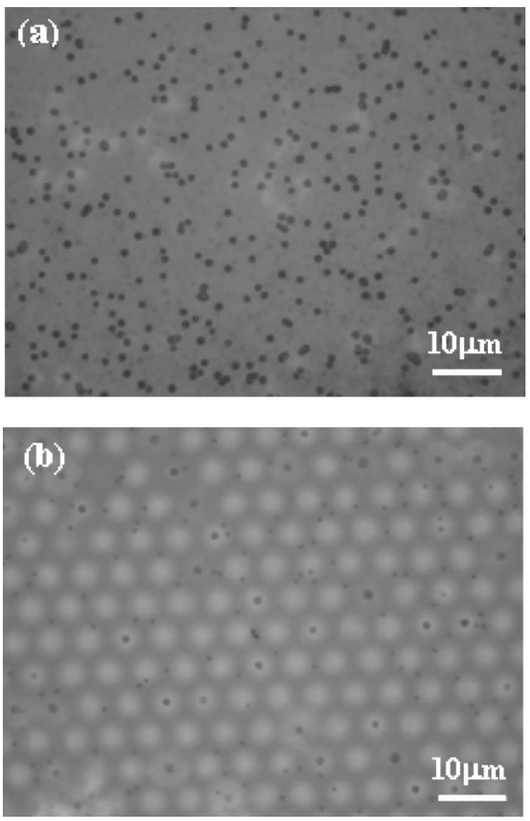

Figure 7. Photographs of the n-GaN etch pits on a (a) conventional sapphire substrate and (b) pyramidal PSS.

EPD estimation. Moreover, it is well known that the near-band-edge luminescence is very sensitive to the dislocation density.[23] Figure 8 shows the room-temperature μ-PL spectra from two regions designated A (epi layer on pyramidal hole) and B (epi layer on flat sapphire). It was found that the luminescence intensity of the on the A region was about 33% higher than that of the B region. The corresponding PL peak energies were 3.419 and 3.424 eV, respectively. The suspended GaN epi layer on the pyramidal hole is believed to be in smaller compressive strain and lower dislocation density, which resulted in a higher luminescence intensity and lower PL peak energy.[24] The redshift of the PL in the GaN areas over the holes in the sapphire could be attributed to a relief of compressive stress in

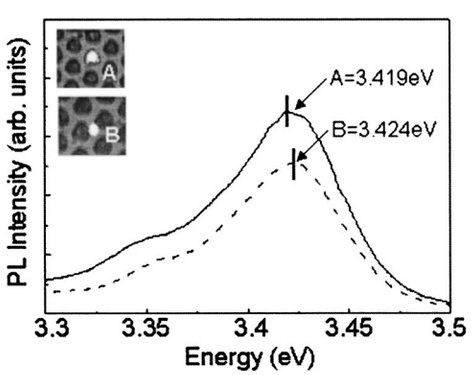

Figure 8. Room-temperature micro photoluminescence spectra of GaN-on-PSS sample from two regions designated A (epi layer on pyramidal hole) and B (epi layer on flat sapphire).

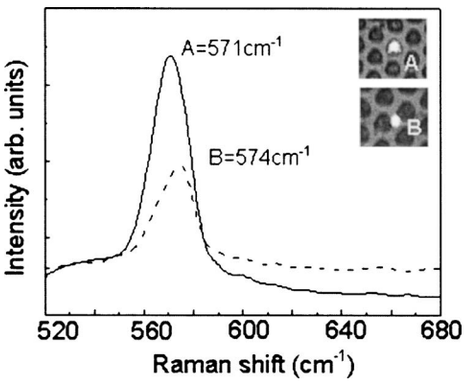

Figure 9. Room-temperature micro Raman spectra of GaN-on-PSS sample from two regions A (epi layer on pyramidal hole) and B (epi layer on flat sapphire).

the GaN. The compressive stress is induced during cooling due to the mismatch in the thermal expansion coefficients between GaN and sapphire. A reduced dislocation density will result in an increase of the total compressive stress at room temperature because dislocations are known to relax stress. The in-grown dislocations directly over substrates can be slightly relaxed stress but will be less relaxed over the hole due to dislocation-free region. Further evidence from the micro Raman results also supports this point. Figure 9 shows the micro Raman spectra from the region A and B, corresponding to 571 and 574 cm^{-1}, respectively. The peak position shifts to lower frequency as a result of the compressive strain relaxation over the holes (region A) in the sapphire.[25] Details of the structural and optical properties of the GaN epi layers grown on a conventional sapphire substrate and a pyramidal PSS are summarized in Table I.

The electroluminescence (EL) spectra of the conventional and pyramidal PSS InGaN LEDs with a 20 mA dc injection current at room temperature are shown in Fig. 10. Both EL peak positions of the pyramidal PSS and conventional LEDs were located at 400 nm. The EL intensity of the pyramidal PSS LED is indicated from a comparison with a conventional LED as higher by about 24.7%. This result indicated that the improvement in EL intensity of the pyramidal PSS LED is attributed to the reduction of dislocation density using PSS. Figure 11 shows the light output power of the conventional and pyramidal PSS LEDs as a function of dc injection current. It can be seen that the output power of both LEDs increased linearly with the injection current up to 100 mA. Under a 20 mA forward injection current, the output power of the conventional and pyramidal PSS LEDs (in epoxy lamp form) were 7.45 and 9.35 mW, respectively. A 25% enhancement in output power can be achieved in the pyramidal PSS LED as compared with that of the conventional LED sample. We attributed the enhanced output power to a combination of improved light extraction efficiency and the reduction in dislocation density using a pyramidal PSS. The improved light extraction efficiency can be further supported by the Trace-Pro simulation data as shown in Fig. 12. Here a 10 mW power (5000 light rays) is assumed to emit randomly from the MQW active layer and the etching depth of the pyramidal hole in PSS is 1.5 μm. The maximum candelas values in both maps were 1.1 and 1.9 mW/sr for

Table I. Summarized optical properties of GaN epi layer grown on both pyramidal PSS and conventional sapphire substrate.

Sample	X-ray fwhm (arcsec)	Etching pits density (cm^{-2})	Micro PL intensity (arb. units)
Conventional sapphire	437.8	1.5×10^{9}	1.27×10^{-6}
Pyramidal PSS	401.4	2.3×10^{8}	1.707×10^{-6}

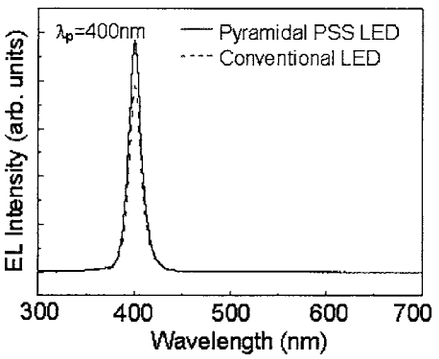

Figure 10. Electroluminescence spectra of InGaN LED samples grown on a conventional sapphire substrate and pyramidal PSS at room-temperature.

the conventional and pyramidal PSS LEDs, respectively. Although the simulation data did not consider the absorption in the epi-structure and the effect from the silver cup in the epoxy lamp form, the present simplified simulation can be used to explain the influence of the optical scattering in the pyramidal PSS. The pyramidal reflector array in the PSS can provide more probability of escaping photons from the GaN/sapphire interface, resulting in an increase in light extracting efficiency. Such a result was also reported by Sun et al.[26]

Conclusions

We described an etching study of the pyramidal PSS using various H_2SO_4/H_3PO_4 mixture ratios. The formation of the crystallographic pyramidal patterns can be attributed to the configuration of surface atoms and bond structure, where the pyramidal pit of the three symmetric sidewall facets were $\{11\bar{2}\bar{k}\}$ on the sapphire (0001) . An evident reduction in dislocation density of the GaN-on-PSS sample can be confirmed by the etch-pit-density, double-crystal X-ray, and micro photoluminescence measurement results. It was found that the EPD was $\sim 1.5 \times 10^9$ cm^{-2} for an n-GaN epi layer on a conventional sapphire substrate and decreased to 2.3×10^8 cm^{-2} for the GaN-on-PSS sample. This indicates that the dislocation reduction can be achieved via the lateral epitaxial overgrowth on a pyramidal PSS. From optical simulation results, the pyramidal reflector array in the PSS was confirmed to provide more probability of escaping photons from the GaN/sapphire interface, making an increase in light extracting efficiency. A 25% enhancement in output power can be achieved in the pyramidal PSS LED as compared with that of the conventional LED sample. The enhanced output power could be due to a combination of improved light extraction efficiency and the reduction in dislocation density using a pyramidal PSS. These results indicate that the wet-etched pyramidal PSSs have high potential for future high-efficiency GaN-based UV-LED applications.

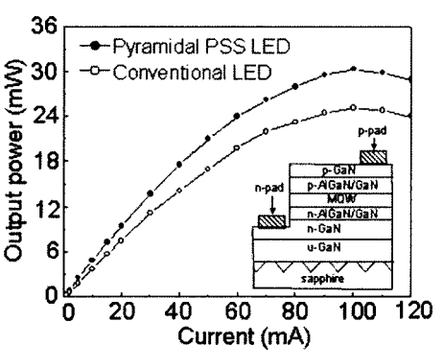

Figure 11. Light output power (λ_D = 400 nm) versus injection current for InGaN LEDs grown on conventional sapphire and pyramidal PSS. The insert shows pyramidal PSS-LED structure.

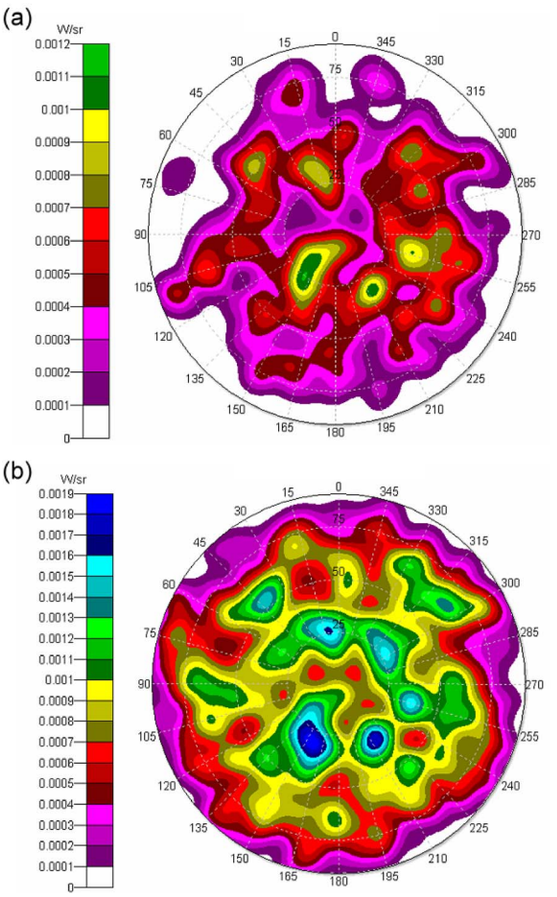

Figure 12. (Color online) Trace-Pro simulation of candela map taken from InGaN LEDs grown on (a) conventional sapphire substrate and (b) pyramidal PSS.

Acknowledgment

This work has been financially supported by the National Science Council (Taipei, Taiwan) and Wafer Works Corp. (Taoyuan, Taiwan) under contract no. NSC 94-2622-E-005-001.

National Chung Hsing University assisted in meeting the publication costs of this article.

References

1. Y. Narukawa, I. Niki, K. Izuno, M. Yamada, Y. Murazki, and T. Mukai, *Jpn. J. Appl. Phys., Part 2*, **41**, L371 (2002).
2. S. X. Jin, J. Li, J. Z. Li, J. Y. Lin, and H. X. Jiang, *Appl. Phys. Lett.*, **76**, 631 (2000).
3. T. Kim, A. J. Danner, and K. D. Choquette, *Electron. Lett.*, **41**, 1138 (2005).
4. T. Fujii, Y. Gao, R. Sharma, E. L. Hu, S. P. DenBaars, and S. Nakamura, *Appl. Phys. Lett.*, **84**, 855 (2004).
5. P. Fini, L. Zhao, B. Moran, M. Hansen, H. Marchand, J. P. Ibbetson, S. P. DenBaars, U. K. Mishra, and J. S. Speck, *Appl. Phys. Lett.*, **75**, 1706 (1999).
6. I. Akasaki, *J. Cryst. Growth*, **198/199**, 885 (1999).
7. M. Iwaya, T. Takeuchi, S. Yamaguchi, C. Wetzel, H. Amano, and I. Akasaki, *Jpn. J. Appl. Phys., Part 1*, **37**, L316 (1998).
8. P. Fini, L. Zhao, B. Moran, M. Hansen, H. Marchand, J. P. Ibbetson, S. P. DenBaars, U. K. Mishra, and J. S. Speck, *Appl. Phys. Lett.*, **75**, 1706 (1999).

9. T. S. Zheleva, O. H. Nam, M. D. Bremser, and R. F. Davis, *Appl. Phys. Lett.*, **71**, 2472 (1997).
10. S. Takumi, S. Hiroki, Y. Katsunori, Y. Masahito, and H. Kazumasa, *J. Cryst. Growth*, **189**, 67 (1998).
11. X. Li, S. G. Bishop, and J. J. Coleman, *Appl. Phys. Lett.*, **73**, 1179 (1998).
12. A. Bell, R. Liu, F. A. Ponce, H. Amano, I. Akasaki, and D. Cherns, *Appl. Phys. Lett.*, **82**, 349 (2003).
13. K. Tadatomo, H. Okagawa, T. Tsunekawa, T. Jyouichi, Y. Imada, M. Kato, H. Kudo, and T. Taguchi, *Phys. Status Solidi A*, **188**, 121 (2001).
14. S. J. Chang, Y. C. Lin, Y. K. Su, C. S. Chang, T. C. Wen, S. C. Shei, J. C. Ke, C. W. Kuo, S. C. Chen, and C. H. Liu, *Solid-State Electron.*, **47**, 1539 (2003).
15. W. K. Wang, D. S. Wuu, S. H. Lin, P. Han, R. H. Hrong, T. C. Hsu, D. C. Huo, M. J. Jou, Y. H. Yu, and A. Lin, *IEEE J. Quantum Electron.*, **41**, 1403 (2005).
16. D. S. Wuu, W. K. Wang, W. C. Shin, R. H. Hrong, C. E. Lee, Y. W. Lin, and J. S. Fang, *IEEE Photon. Technol. Lett.*, **17**, 288 (2005).
17. M. Kappelt and D. Bimberg, *J. Electrochem. Soc.*, **143**, 3271 (1996).
18. F. Dwikusuma, D. Saulys, and T. F. Kuech, *J. Electrochem. Soc.*, **149**, G603 (2002).
19. K. C. Chou, K. Hsu, P. C. Teng, C. Hsu, T. Y. Chou, F. H. Kan, and J. Y. Chu, *J. Chin. Ceram. Soc.*, **27**, 727 (1999).
20. W. Kern, *RCA Rev.*, **39**, 278 (1978).
21. S. Srinivasan, M. Stevens, F. A. Ponce, and T. Mukai, *Appl. Phys. Lett.*, **87**, 131911 (2005).
22. B. Beaumont, Ph. Vennéguès, and P. Gibart, *Phys. Status Solidi A*, **227**, 1 (2001).
23. L. Macht, J. L. Weyher, A. Grzegorczyk, and P. K. Larsen, *Phys. Rev. B*, **71**, 073309 (2005).
24. L. Macht, P. R. Hageman, S. Haffouz, and P. K. Larsen, *Appl. Phys. Lett.*, **87**, 131904 (2005).
25. D. Wang, S. Jia, K. J. Chen, K. M. Lau, Y. Dikme, P. van Gemmern, Y. C. Lin, H. Kalisch, R. H. Jansen, and M. Heuken, *J. Appl. Phys.*, **97**, 056103 (2005).
26. C. C. Sun, C. Y. Lin, T. X. Lee, and T. H. Yang, *Opt. Eng.*, **43**, 1700 (2004).